Supporting Information

Cao et al. 10.1073/pnas.1208324109

Among tumor-produced known angiogenic factors, members in the VEGF and FGF families are relatively well characterized. The VEGF family consists of five structurally related members including VEGF-A, VEGF-B, VEGF-C, VEGF-D, and PlGF (1–3). Although virtually all VEGF members are involved in modulation of angiogenesis, VEGF-C is defined as a potent lymphangiogenic factor that directly acts on lymphatic endothelial cells (LECs) via interaction with the VEGFR-3 receptor (4). The VEGF-C plus VEGFR-3 system is essentially required for embryonic development and deletion of either VEGF-C or VEGFR-3 leads to embryonic lethality owing to defective lymphangiogneis and malformation of blood vessels (5). VEGF-A is also a potent lymphangiogenic factor and its lymphangiogenic activity is mainly mediated through VEGFR-2 receptor (6–10). Similar to VEGF-C, VEGF-D, binds to VEGFR-3 that transduces proliferation and migration signals in LECs, leading to potent lymphangiogenic activity in vivo (11). Overexpression of VEGF-C in various tumors promotes intratumoral lymphangiogenesis and lymphatic metastasis (12–14). The FGF family consists of a large number of structurally and functionally related proteins that display biological functions via interactions with four tyrosine kinase receptors (i.e., FGFR-1, -2, -3, and -4) (15). FGF-2, the prototype of FGFs, is widely distributed in most cell types in the body and is capable to bind all four FGFRs.

SI Discussion

Similar to the process of blood vessel formation, lymphangiogenesis is a complex and multistep process that is tightly regulated by several lymphangiogenic factors (1, 16, 17). The VEGF-C/-D plus VEGFR-3 signaling system plays an essential role in the initial formation of the embryonic lymphatic system, in triggering lymphangiogenic responses during physiological and pathological conditions, and in maintenance of the lymphatic integrity and functions (1, 13, 18). As a result, deletion of either the *Vegfr-3* or *Vegf-c* gene in mice leads to early embryonic lethality owing to defective development of the lymphatic system (5). Comparable to the VEGF-A plus VEGFR-2 system, the VEGF-C/-D plus VEGFR-3 signaling controls the switch between tip and stalk endothelial cells of blood vessels in association with the notch signaling system (19). Although the switch of endothelial cell types between tip and stalk by the VEGF signaling system is relatively well studied, the essential role of the VEGF-C/-D plus VEGFR-3 signaling in controlling lymphatic vessel growth in response to other growth factors has not been studied. One of the key structural differences between blood vessels and lymphatics is the composition of extracellular matrix and the basement membrane (1). Unlike the blood vasculature, lymphatic vessels generally lack the coverage of perivacular cells including pericytes and vascular smooth muscle cells that prevent excessive and undirected endothelial tip formation (20). The exact mechanism by which LECs form tips from the leading front of growing lymphatics without activation of the neighboring stalk cells is not understood.

SI Experimental Procedures

Reagents and Ethical Permits. SiRNA targeting *Fgfr-1*, scrambled siRNA and NTER transfecting medium were purchased from Sigma. Recombinant human FGF-2 (rhFGF-2) was obtained from Sigma or Pharmacia and Upjohn and rhVEGF-C was purchased from R&D Systems or Peprotech. Antibodies used in this study include: a rat anti-mouse CD31 antibody (BD-Pharmingen); a hamster anti-mouse CD31 (Millipore) antibody; a rabbit anti-mouse lymphatic vessel endothelial hyaluronan receptor-1 (LYVE-1) (AngioBio) antibody; a FGFR-1 neutralizing antibody (IMC-A1; ImClone); a rat anti-mouse VEGFR-3 antibody (mF4-31C1; ImClone), and a goat anti-mouse VEGFR-3 antibody (R&D Systems); an Alexa Fluor-488–conjugated donkey anti-rabbit antibody (Invitrogen); an Alexa Fluor-555–conjugated goat anti-rat antibody (Invitrogen); a Cy3-conjugated donkey anti-goat antibody (Jackson ImmunoResearch); a Cy5-conjugated goat anti-rabbit antibody (Chemicon); and a Cy3-conjugated goat anti-hamster antibody (Jackson ImmunoResearch). Female or male C57BL/6 or immunodefecient SCID mice at the age of 6–8 wk were used for our study. All animal studies were approved by the Northern Stockholm Experimental Animal Ethical Committee.

Cell Lines. Human TERT-HDLECs (hTERT-immortalized human dermal LECs) (21), an immortalized human LEC (hLEC) line, was kindly provided by Michael S. Pepper, University of Pretoria, Pretoria, South Africa. Primary mouse LECs (mLECs) were isolated from lung tissues of C57BL/6 mice. Briefly, freshly dissected lung tissues were cut into small pieces, followed by digestion with 0.2% collagenase. Single cell suspensions were cultured with EGM2 medium (Lonza Clonetics) supplemented with 10% (vol/vol) FCS. LYVE-1^+ cells were sorted and collected by FACS. LYVE-1^+ LEC cells were used for experimental analysis. Both hLECs and mLECs were manintained and cultured in gelatin-coated tissue culture flasks in endothelial cell growth medium MV2 (Promocell) supplemented with 200 U/mL penicillin and 50 μg/mL streptomycin.

Signal Tansduction Assays. Human TERT-HDLECs were grown to 90% confluency in gelatin-coated 60-mm dishes, washed with PBS and incubated for 60 min in serum-free medium (MV2 from Promocell). After stimulation with 50 ng/mL FGF-2 or 50 ng/mL VEGF-C for up to 60 min, cells were lyzed with a NUPAGE LDS sample buffer (Invitrogen) containing a mixture of protease and phosphatase inhibitors (aprotinin, leupeptin, pepstatin, vanadate, NaF, and PMSF). An equal amount of protein samples was separated by SDS/PAGE (10% BIS-Tris gel; Invitrogen) and specific proteins were detected by Western blotting. Antiphosphorylated Akt (Ser473) and antiphosphorylated ribosomal protein S6 (Ser235/236) antibodies were purchased from Cell Signaling Technology, antiphosphorylated ERK1/2 (Thr202/Tyr204) was from Santa Cruz, and anti-GAPDH antibody was purchased from Millipore.

RT-PCR. Reverse transcription was performed using total RNA extracted from hTERT-HDLECs and the Omniscript Reverse Transcriptase kit (Qiagen Nordic). A specific cDNA coding for a 274-bp *Fgfr-1* fragment was amplified by PCR using the following pairs of primers: 5′-ACGGCAGCATCAACCACAC-3′ (forward primer) and 5′-TGAAGCACCTCCATCTCTTTGTC-3′ (reverse primer).

Quantitative PCR Analysis. Human TERT-HDLECs were grown to 70–80% confluency followed by starvation for 24 h before stimulation with growth factors. Cells were stimulated with 10 ng/mL FGF-2 or VEGF-C for 24 or 48 h before RNA extraction. Total RNA was extracted using a GeneJET RNA Purification Kit (Fermentas) and cDNA was synthesized using a RevertAid H Minus First Strand cDNA Synthesis Kit (Fermentas) according to the manufacturer's protocols. The thermal conditions for cDNA synthesis consisted of initial incubation at 25 °C for 5 min, followed by further incubation at 42 °C for 60 min and termi-

nation at 70 °C for 5 min. The synthesized cDNA samples were kept at –20 °C until further use. Quantitative PCR were performed using a protocol consisting of 2-min preincubation at 50 °C, 10-min initial denaturation at 95 °C, followed by 40 cycles consisting of 15 min at 95 °C, 1 min at 60 °C, and 1 min at 72 °C. Following pairs of primers were used: *hFgfr1*: forward primer, 5′-CATCACGGCTCTCCTCCAGT-3′; reverse primer, 5′-AGGGGTTTGCCTAAGACCAG-3′; *hVegfr3*: forward primer, 5′-CAACAGACCCACACAGAACT-3; and reverse primer, 5-TTTCCATCCTTGTACCACTG-3.

Migration Assay. A previously described a modified Boyden chamber technique was used to study the ability of isolated primary mLECs to migrate through a micropore nitrocellulose filter (8-μm pore size) (22). In brief, angiogenic factors (FGF-2 or VEGF-C) at the concentration of 100 ng/mL in 5% (vol/vol) FCS-basal MV2-medium were added to the lower chamber. Approximately 30,000 mLECs in serum-free basal MV2-medium containing 1 μg/mL FGFR-1 neutralizing antibody or a rat anti-mouse VEGFR-3 neutralizing antibody were seeded to each well of the upper chamber. Cells were incubated overnight and transmigrated cells underneath the filter were fixed with methanol, followed by staining with a Giemsa solution and counted using a light microscope. The data were quantified by scoring the average number of six replicates from each sample. The experiments were repeated twice.

Cell Proliferation Assay. MTT [3-(4,5-Dimethylthiazol-2-yl)-2,5-Diphenyltetrazolium Bromide]-based proliferation assay was used for our study. Briefly, 1,000 hTERT-HDLECs were seeded onto each well of gelatin-coated 96-well plates in a total volume of 200 μL medium containing 2% (vol/vol) FCS for 4–6 d. Cells were treated with or without FGF-2 (50 ng/mL) and/or VEGF-C (50 ng/mL) at day 1 and renewed at day 3. siRNA experiments were performed by transfecting cells at day 1 with 30 nM siRNA targeting *Fgfr-1* or scrambled siRNA. Cells were stimulated 2 d after transfection. Proliferation was measured on 3 or 6 d after stimulation using the EZ4U-proliferation Kit (Biomedica) based on the method of reduction of tetrazolium salt to colored formazan. Samples were incubated 3 h with substrate before measurement of absorbance at 450 nm with 630 nm as background. For mLEC proliferation assay, ~3,000 mLECs were placed onto each well of the gelatin-coated 96-well plates in a total volume of 200 μL of basal MV2-medium containing 2% (vol/vol) FCS, followed by incubation for 24 h. Cells were treated with 100 ng/mL recombinant FGF-2 or VEGF-C in the presence or absence of 1 μg/mL FGFR-1 or VEGFR-3 blockade. Untreated cells were used as negative controls. After incubation at 37 °C for 72 h, 20 μl MTT (5 mg/mL) was added to each well and samples were further incubated for 4 h. The absorbance of the purple formazan solution at wavelength of 490 nm was measured ($n = 6$ per group).

Mouse Corneal Micropocket Assay. The mouse corneal micropocket assay was performed in C57BL/6 mice as previously described (23–25). In brief, a polymer micropellet containing 40 ng of FGF-2 or 160 ng of VEGF-C was implanted into each corneal micropocket, which was surgically created on a single eye of each animal (five to six mice per group). In combination studies, FGF-2 and VEGF-C were coimplanted into each micropocket (five to six mice per group). Corneal neovascularization was measured on day 6 after pellet implantation. The treatment of neutralizing antibodies was performed as previously described (26).

Mouse Tumor Model. Approximately 1×10^6 tumor cells from vector-, FGF-2–, or VEGF-C–transfected clones were subcutaneously implanted in the central position along the dorsal midline of each immunodeficient SCID mouse (six mice per group). Half-numbers of FGF-2– and VEGF-C–tumor cells were mixed for coimplantation experiments (six mice per group). Tumor growth was measured every other day and tumor volumes were calculated according to a standard formula as previously described (22, 25, 27).

Metastasis Assay. When primary tumors grew to a volume of ~1.5 cm^3 (within the ethical limit), primary tumors and residue surrounding tissues were surgically removed under anesthetic conditions. Open wounds were sutured and mice were given pain killer in two consecutive days (Temgesic, 0.1 mg/kg, twice a day). Typically, visible sentinel lymph node metastases were detectable in bilateral subaxillary lymph nodes of VEGF-C– or FGF-2 plus VEGF-C tumor-bearing mice after two weeks. At this time point, tumor-bearing mice from all groups (six mice per group) were killed and various organs, including lymph nodes, lung, liver, spleen, kidney, and brain were collected from each mouse for histological analysis.

Histology. Paraffin-embedded tissue samples were sectioned at 4-μm thickness, followed by staining with H&E using a standard protocol (27).

Whole-Mount Immunostaining. Whole-mount staining was performed according to our previously described methods (22, 24). Mouse corneas were dissected and flat-mounted according to our published protocols (24). For example, corneal, tumor, and lymph node tissues were usually double immunostained with rat anti-mouse CD31 monoclonal antibody (BD Pharmingen) and rabbit anti-mouse LYVE-1 antibody (AngioBio). A goat anti-rat Alexa Fluor-555–conjugated antibody (Invitrogen) and a Cy3-conjugated goat anti-rabbit IgG antibody (Chemicon) were used as secondary antibodies. Immunostained positive signals and EGFP positive tumor cells were detected using a Nikon C1 Confocal microscope (Nikon) or a Zeiss Confocal LSM510 microscope (Carl Zeiss). For 3D images of each dataset, scanning five to six layers were assembled using a confocal microscope software program (EZ-C1).

1. Alitalo K, Carmeliet P (2002) Molecular mechanisms of lymphangiogenesis in health and disease. *Cancer Cell* 1:219–227.
2. Cao Y (2009) Positive and negative modulation of angiogenesis by VEGFR1 ligands. *Sci Signal* 2:re1.
3. Ferrara N, Kerbel RS (2005) Angiogenesis as a therapeutic target. *Nature* 438:967–974.
4. Joukov V, et al. (1997) Proteolytic processing regulates receptor specificity and activity of VEGF-C. *EMBO J* 16:3898–3911.
5. Haiko P, et al. (2008) Deletion of vascular endothelial growth factor C (VEGF-C) and VEGF-D is not equivalent to VEGF receptor 3 deletion in mouse embryos. *Mol Cell Biol* 28:4843–4850.
6. Nagy JA, et al. (2002) Vascular permeability factor/vascular endothelial growth factor induces lymphangiogenesis as well as angiogenesis. *J Exp Med* 196:1497–1506.
7. Cursiefen C, et al. (2004) VEGF-A stimulates lymphangiogenesis and hemangiogenesis in inflammatory neovascularization via macrophage recruitment. *J Clin Invest* 113: 1040–1050.
8. Hirakawa S, et al. (2005) VEGF-A induces tumor and sentinel lymph node lymphangiogenesis and promotes lymphatic metastasis. *J Exp Med* 201:1089–1099.
9. Björndahl MA, et al. (2005) Vascular endothelial growth factor-a promotes peritumoral lymphangiogenesis and lymphatic metastasis. *Cancer Res* 65:9261–9268.
10. Cao R, et al. (2004) Comparative evaluation of FGF-2-, VEGF-A-, and VEGF-C-induced angiogenesis, lymphangiogenesis, vascular fenestrations, and permeability. *Circ Res* 94:664–670.
11. Mäkinen T, et al. (2001) Inhibition of lymphangiogenesis with resulting lymphedema in transgenic mice expressing soluble VEGF receptor-3. *Nat Med* 7:199–205.
12. Cao Y (2005) Direct role of PDGF-BB in lymphangiogenesis and lymphatic metastasis. *Cell Cycle* 4:228–230.
13. Skobe M, et al. (2001) Induction of tumor lymphangiogenesis by VEGF-C promotes breast cancer metastasis. *Nat Med* 7:192–198.
14. Beasley NJ, et al. (2002) Intratumoral lymphangiogenesis and lymph node metastasis in head and neck cancer. *Cancer Res* 62:1315–1320.
15. Auguste P, Javerzat S, Bikfalvi A (2003) Regulation of vascular development by fibroblast growth factors. *Cell Tissue Res* 314:157–166.
16. Cao Y (2005) Opinion: emerging mechanisms of tumour lymphangiogenesis and lymphatic metastasis. *Nat Rev Cancer* 5:735–743.

17. Stacker SA, Achen MG, Jussila L, Baldwin ME, Alitalo K (2002) Lymphangiogenesis and cancer metastasis. *Nat Rev Cancer* 2:573–583.
18. Oliver G, Harvey N (2002) A stepwise model of the development of lymphatic vasculature. *Ann N Y Acad Sci* 979:159–165, discussion 188–196.
19. Tammela T, et al. (2011) VEGFR-3 controls tip to stalk conversion at vessel fusion sites by reinforcing Notch signalling. *Nat Cell Biol* 13:1202–1213.
20. Petrova TV, et al. (2004) Defective valves and abnormal mural cell recruitment underlie lymphatic vascular failure in lymphedema distichiasis. *Nat Med* 10:974–981.
21. Nisato RE, et al. (2004) Generation and characterization of telomerase-transfected human lymphatic endothelial cells with an extended life span. *Am J Pathol* 165:11–24.
22. Nissen LJ, et al. (2007) Angiogenic factors FGF2 and PDGF-BB synergistically promote murine tumor neovascularization and metastasis. *J Clin Invest* 117:2766–2777.
23. Cao R, et al. (2003) Angiogenic synergism, vascular stability and improvement of hind-limb ischemia by a combination of PDGF-BB and FGF-2. *Nat Med* 9:604–613.
24. Cao R, et al. (2011) Mouse corneal lymphangiogenesis model. *Nat Protoc* 6:817–826.
25. Cao R, et al. (2010) VEGFR1-mediated pericyte ablation links VEGF and PlGF to cancer-associated retinopathy. *Proc Natl Acad Sci USA* 107:856–861.
26. Kubo H, et al. (2002) Blockade of vascular endothelial growth factor receptor-3 signaling inhibits fibroblast growth factor-2-induced lymphangiogenesis in mouse cornea. *Proc Natl Acad Sci USA* 99:8868–8873.
27. Eriksson A, et al. (2002) Placenta growth factor-1 antagonizes VEGF-induced angiogenesis and tumor growth by the formation of functionally inactive PlGF-1/VEGF heterodimers. *Cancer Cell* 1:99–108.

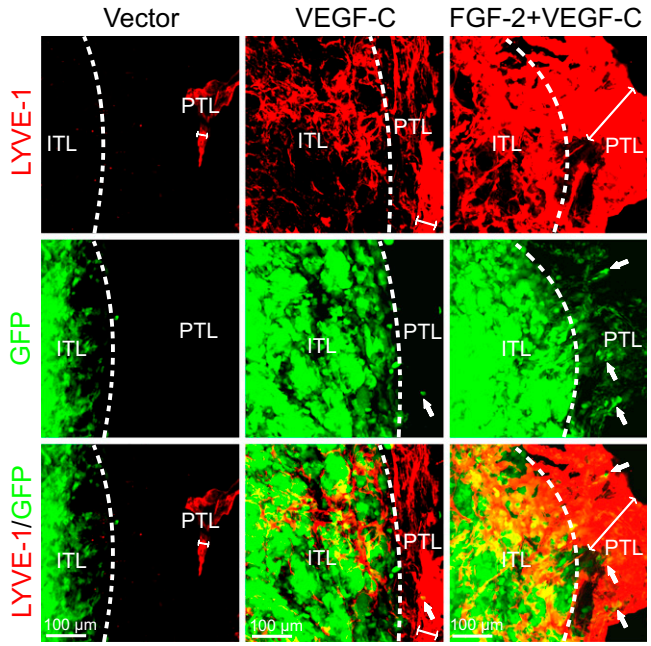

Fig. S1. Tumor lymphangiogenesis and tumor cell dissemination. Intratumoral and peritumoral lymphatic (ITL and PTL) vessels in mice bearing various tumors were detected using LYVE-1–specific staining. Dashed lines mark the borders between the tumor edge and surrounding healthy tissues. Solid line with double arrows mark the diameter of PTL. Arrows point to the disseminated $EGFP^+$ tumor cells in PTLs of VEGF-C and FGF-2 plus VEGF-C tumor-bearing mice.